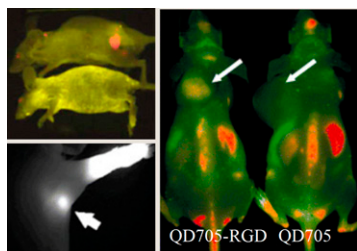**Connecting the quantum dots:** Bentolila and colleagues provide an overview of the growing contributions of quantum dots to in vivo molecular imaging in small-animal models and describe the possibilities for clinical applications and novel hybrid approaches. . . . . ***Page 493***

QD705-RGD QD705

Toward routine vulnerable plaque imaging: Fox and Strauss offer a perspective on the current status of metabolic imaging of vulnerable plaque in coronary arteries and preview an article on this topic in this issue of *JNM*. . . . . ***Page 497***
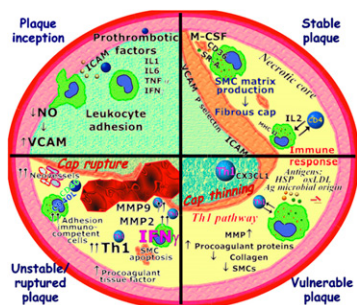

Testing a PET/CT cocktail: Iagaru and colleagues report on the combined administration of ^{18}F and ^{18}F-FDG in a single PET/CT study for cancer detection in a range of malignancies. . . . . . . ***Page 501***
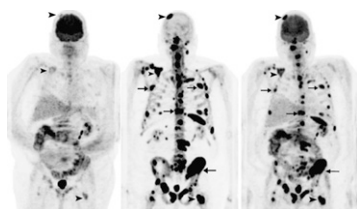

PET/CT evaluation of ascites: Zhang and colleagues compare ^{18}F-FDG PET/CT with CT alone in determining the unknown primary cause of ascites and in detecting abdominal cavity metastases. . . . . ***Page 506***
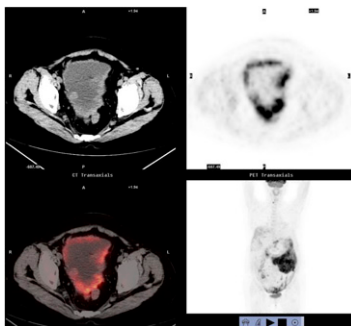

^{18}F-FDOPA PET for pheochromocytomas: Imani and colleagues investigate the sensitivity and specificity of PET with ^{18}F-FDOPA as an independent marker for diagnosis and localization of benign and malignant pheochromocytomas. . . . . ***Page 513***
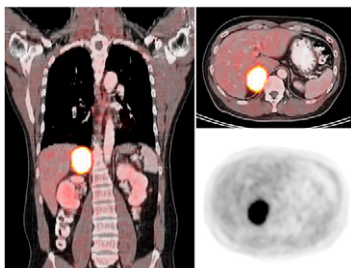

Segmented attenuation maps for PET/MRI: Martinez-Möller and colleagues propose and evaluate a potential solution to the challenge of attenuation correction of whole-body PET data in combined PET/MRI. . . . . ***Page 520***
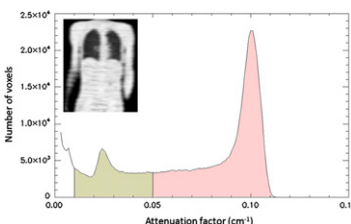

PET in diffuse large B-cell lymphoma: Itti and colleagues determine whether semiquantification of standardized uptake values improves the prognostic value of ^{18}F-FDG PET after 4 cycles of chemotherapy for diffuse large B-cell lymphoma. . . . . ***Page 527***
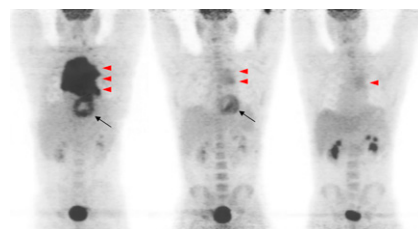
Annexin imaging of joint prostheses: Lorberboym and colleagues explore the use of ^{99m}Tc-recombinant human annexin V imaging for differential diagnosis of aseptic loosening and low-grade infection in hip and knee prostheses. . . . . ***Page 534***

Ant   Post
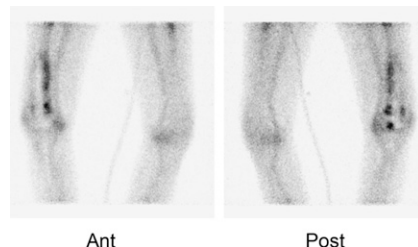
PET/CT in chronic lung disease: Groves and colleagues evaluate integrated ^{18}F-FDG PET/CT in idiopathic pulmonary fibrosis and other forms of diffuse parenchymal lung disease and assess patterns of tracer metabolism in these patients. . . . . ***Page 538***
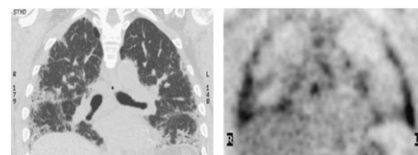

SPECT in stable ischemic heart disease: Gimelli and colleagues compare the capabilities of gated stress/rest myocardial perfusion SPECT with those of a complete diagnostic work-up and other indicators in predicting cardiac events in patients with stable ischemic heart disease. . . . . ***Page 546***

Half-time SPECT MPI with AC: Ali and colleagues describe a new algorithm and post-processing technique facilitating half-time gated myocardial SPECT perfusion imaging with attenuation correction. . . . . . . ***Page 554***

**PET/CT imaging of coronary plaque:** Wykrzykowska and colleagues report on

^{18}F-FDG PET/CT imaging of inflamed and vulnerable plaque in coronary arteries using a low-carbohydrate, high-fat preparation in patients with suppression of myocardial uptake. . . . . ***Page 563***
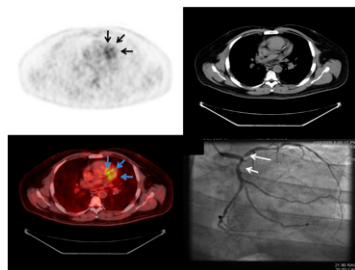
Radiotracer breast cancer imaging: Lee and colleagues provide the first in a 2-part educational overview of current and future radiotracer imaging methods for breast cancer in the context of management strategies and non-nuclear imaging approaches. . . . . . ***Page 569***
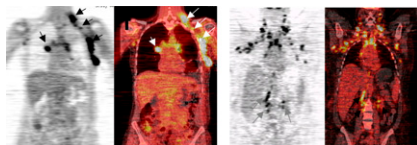

Antisense-mediated Auger cytotoxicity: Liu and colleagues evaluate a novel 3-component streptavidin-delivery nanoparticle capable of tumor targeting, transmembrane transport, ^{111}In nuclear migration, and specific radiation-induced cytotoxicity. . . . . ***Page 582***
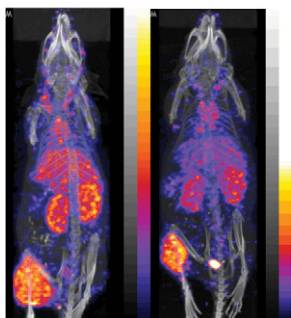

Side-chain coordination in HYNIC peptides: King and colleagues determine the effects of assisted coordination by amino acids, such as histidine and glutamic acid, on the function of ^{99m}Tc-labeled gastrin peptide–HYNIC conjugates in targeting cholecystokinin-R in small-animal models. . . . .***Page 591***

U-SPECT-II rodent imaging system: van der Have and colleagues describe a new SPECT device that enables both molecular imaging of murine organs down to resolutions of less than 0.5 mm and high-resolution total-body imaging. . . . .***Page 599***
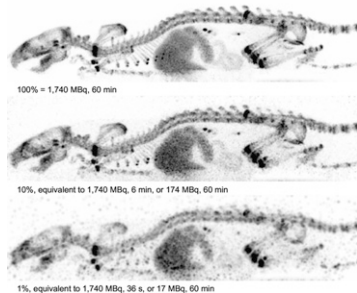
PET imaging with anti-PSMA antibody: Elsässer-Beile and colleagues elucidate the in vivo behavior and tumor uptake of a radiolabeled anti–prostate-specific membrane antigen monoclonal antibody and review its potential as a PET tracer. . . . .***Page 606***
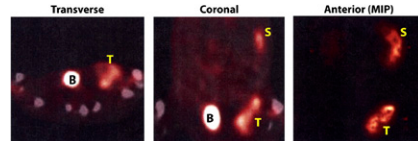
MMP imaging in atherosclerotic mice: Ohshima and colleagues detail a strategy for noninvasive assessment of the extent of matrix metalloproteinase expression in various transgenic mouse models of atherosclerosis. . . . .***Page 612***
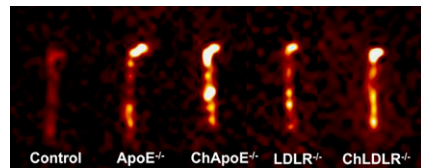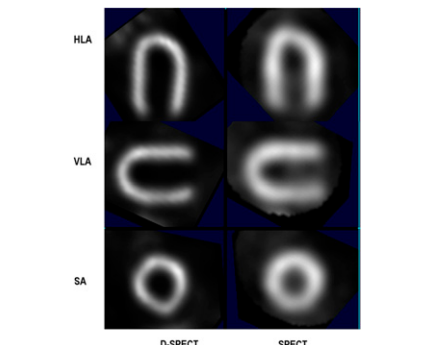

Fibronectin stimulates ^{18}F-FDG uptake: Paik and colleagues investigate the mechanisms by which matrix fibronectin influences endothelial cell glucose uptake and describe the signaling pathways that mediate this effect. . . . . ***Page 618***

LLP2A tumor targeting: DeNardo and colleagues review the design, synthesis, radiolabeling, and in vivo pharmacokinetics of derivatives of a high-affinity, high-specificity peptidomimetic ligand that binds the activated $\alpha_4\beta_1$ integrin found on a variety of malignant lymphoid cell lines. . . . .***Page 625***
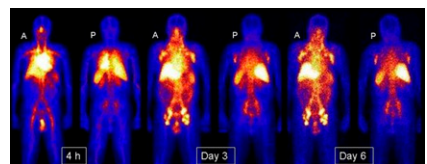

Solid-state single-photon imaging: Gambhir and colleagues report on the development and validation, including patient scanning, of a new solid-state single-photon γ-camera and compare it with a conventional SPECT Anger camera. . . . .***Page 635***

Ibritumomab tiuxetan dose estimate: Fisher and colleagues evaluate organ radiation absorbed doses from intravenously administered [111]In- and ^{90}Y-ibritumomab tiuxetan, as published in MIRD Dose Estimate Report No. 20. . . . .***Page 644***

ON THE COVER

This rest/stress ^{99m}Tc-tetrofosmin SPECT study compares 2 acquisition methods. At top is a full-time acquisition reconstructed with ordered-subset expectation maximization without attenuation correction; at bottom is a half-time acquisition reconstructed with ordered-subset expectation maximization and resolution recovery with attenuation correction. No difference in image quality or clinical diagnosis was observed in 96% of cases between the 2 methods.